Investigation of Surface Segregation in Fe-Cr-Si Alloys by XPS

K. IDCZAK and R. IDCZAK

The surface segregation of Fe-Cr-Si alloys was studied using the X-ray photoelectron spectroscopy (XPS). The experiment was performed in two stages, for the as-prepared samples and after oxidation process. Analysis of measured XPS spectra allowed one to characterize the changes in the surface chemical composition during the oxidation and thermal treatment procedures. According to the obtained results, it could be stated that the enhanced anti-corrosion properties of the Fe-Cr-Si alloys which contain more than 10 at. pct of Cr and 5 at. pct of Si in the bulk are mainly connected with the strong surface segregation process of both solutes. In the case of alloys which contain less solutes ($Fe_{0.94}Cr_{0.03}Si_{0.03}$, $Fe_{0.90}Cr_{0.05}Si_{0.05}$), the behavior of Cr atoms is different during the oxidation process. Chromium does not segregate to the surface, instead it diffuses into deeper parts of the material leaving the surface covered only by silicon and iron oxides. This effect is responsible for much worse corrosion resistance of the $Fe_{0.94}Cr_{0.03}Si_{0.03}$ and $Fe_{0.90}Cr_{0.05}Si_{0.05}$ alloys.

https://doi.org/10.1007/s11661-020-05758-5

I. INTRODUCTION

IRON alloys, including steels, have been intensively studied for years because of their importance as structural materials for the modern industry. Currently, one of the main challenges in this field is related to understand the processes associated with atmospheric and high-temperature corrosion.[1–3] In order to reduce the negative effect of corrosion on the global economy, many researchers are still conducting intensive work to improve the anti-corrosive properties of iron and its alloys with a low content of other elements. The corrosion-resistant properties of these multi-component alloys depend mainly on the surface oxidation mechanism and the ability of alloy surface to form passive films which act as a barrier to additional oxidation reaction in the deeper parts of material. One of the most important physical phenomena which is responsible for the formation of passive films in iron-based alloys is the surface segregation process.[4–9] Due to this process, a very small concentration of solute atoms in the bulk of the material can lead to a very significant coverage of these atoms on a free surface of the alloy.

As it was shown previously,[10–16] the addition of Cr and/or Si atoms to α-Fe drastically reduces the oxidation process of iron atoms during exposure to air at high temperature. In particular, the results obtained by the ^{57}Fe transmission Mössbauer spectroscopy (TMS) as well as by the conversion electron Mössbauer spectroscopy (CEMS) for the $Fe_{0.85}Cr_{0.10}Si_{0.05}$ alloy indicate that the high-temperature atmospheric corrosion of this material is almost stopped at 870 K and 1070 K.[16] The most plausible explanation of this behavior could be linked to the strong segregation process of Si and/or Cr atoms to the alloy surface. However, in a study by Idczak,[16] that suggestion is rather speculative since it requires confirmation by surface-sensitive experimental techniques. An extremely useful tool for this purpose is the X-ray photoelectron spectroscopy (XPS). This experimental technique collects data from a surface layer of a few nanometers and provides detailed information about atomic concentration of selected elements as well as types of atomic bonds which are present on the surface of studied material.[17] Moreover, the XPS experiments which were performed for Fe-Cr [4, 14] and Fe-Si [7, 15] systems gave clear evidence that the enhanced anti-corrosion behavior of these binary alloys is connected with the surface segregation of Cr and Si atoms. Taking the above into account, this work is mainly focused on determination of the influence of the surface segregation process on the corrosion resistance properties of ternary Fe-Cr-Si alloys. Four polycrystalline Fe-Cr-Si alloys were investigated by XPS in order to estimate the changes in surface chemical composition caused by oxidative annealing in air at high temperature

K. IDCZAK is with the Institute of Experimental Physics, University of Wroclaw, pl. M. Borna 9, 50-204 Wroclaw, Poland. Contact e-mail: kidczak@ifd.uni.wroc.pl R. IDCZAK is with the Institute of Experimental Physics, University of Wroclaw and also with the Institute of Low Temperature and Structure Research, Polish Academy of Science W. Trzebiatowski Institute, ul. Okólna 2, 50-422 Wroclaw, Poland

Manuscript submitted November 6, 2019.
Article published online April 19, 2020

as well as by rapid thermal annealing at various temperatures in vacuum. An insight into corrosion properties of the Fe-Cr-Si alloy is presented in correlation with recently obtained Mössbauer data.[16]

II. EXPERIMENTAL

The samples of $Fe_{0.94}Cr_{0.03}Si_{0.03}$, $Fe_{0.90}Cr_{0.05}Si_{0.05}$, $Fe_{0.85}Cr_{0.10}Si_{0.05}$, and $Fe_{0.80}Cr_{0.15}Si_{0.05}$ alloys were prepared in an arc furnace. Appropriate amounts of the 99.98 pct pure iron, 99.995 pct pure chromium, and 99.95 pct pure silicon were melted in a water-cooled copper crucible under argon atmosphere and quickly cooled to room temperature. Solidified alloys were remelted two times to ensure homogeneity. The weight losses during the melting process were below 0.2 pct of the original weight, so it could be assumed that the chemical composition of the obtained ingots is close to nominal ones. In the next step, the resulting ingots were cold-rolled to the final thickness of about 0.10 mm. Finally, the foils were annealed in the vacuum at 1270 K for 2 hours. The base pressure during the annealing procedure was lower than 10^{-4} Pa. To obtain homogeneous and defect free samples,[18] after the annealing process, the foils were slowly cooled to room temperature during 6 hours. After that preparation, the samples were divided into two groups. The first were alloys annealed only in vacuum (named "as prepared") and the second were additionally exposed to air at 870 K for 2 hours (named "oxidized"). During exposure to air, the ambient humidity was monitored using hair hygrometer and it was in the range from 45 pct RH to 65 pct RH.

The quality of prepared samples was checked by TMS. The obtained ^{57}Fe Mössbauer spectra were similar to those presented in Idczak's work [16] indicating that all prepared Fe-Cr-Si alloys were in a single phase with body-centered cubic (bcc) structure. This finding is in agreement with Fe-Cr-Si phase diagrams presented in the work by Cui and Jung.[19]

All samples were placed in the ultrahigh-vacuum (UHV) apparatus, with a pressure about 4×10^{-8} Pa, equipped with the XPS analyzer (Phoibos 150) with Mg Kα and Al Kα X-ray sources. The measurements were performed in conditions similar to those described in Reference 11. The highest temperature at which the samples were annealed in UHV was 1300 K. According to the Fe-Cr-Si phase diagrams,[19] all studied alloys are stable in the bcc structure up to 1300 K. Therefore, it is plausible to assume that any potential changes in the surface chemical composition which may occur during annealing in UHV cannot be induced by structural phase transitions or formation of new intermetallic phases in the bulk of studied alloys.

Obtained spectra were analyzed using the CasaXPS program. The background of spectra was subtracted using a software based on Shirley method. Fitting method was the Gaussian–Lorentzian (GL(30 pct)). For Fe 2p envelope analysis, the Gupta–Sen multiplet peaks (GS) fitting method was used.[20]

III. RESULTS

The XPS technique was used to study the chemical composition and surface atomic concentrations of selected elements. The surface atomic concentration c_i of selected elements were estimated according to the following formula:

$$c_i = \frac{I_i/\sigma_i \cdot \lambda_i}{\sum I_j/\sigma_j \cdot \lambda_j} \times 100 \text{ pct}, \quad [1]$$

where I_i is a selected XPS peak intensity (Fe $2p_{3/2}$, Cr $2p_{3/2}$, Si 2p, O 1s, and C 1s), σ is a photoionization cross section for selected element (Scofield parameter),[21] and λ is a inelastic mean free path of electrons with a certain kinetic energy related to the selected XPS core-level line.[22] The presented c_i values have an uncertainty of less than 2 pct.

A. *$Fe_{0.94}Cr_{0.03}Si_{0.03}$ Alloy*

Figure 1 presents the surface atomic concentration of selected elements obtained for the as-prepared and oxidized $Fe_{0.94}Cr_{0.03}Si_{0.03}$ samples after annealing at various temperatures. Figure 2 presents the selected XPS spectra for the same samples after final annealing at 1300 K in UHV.

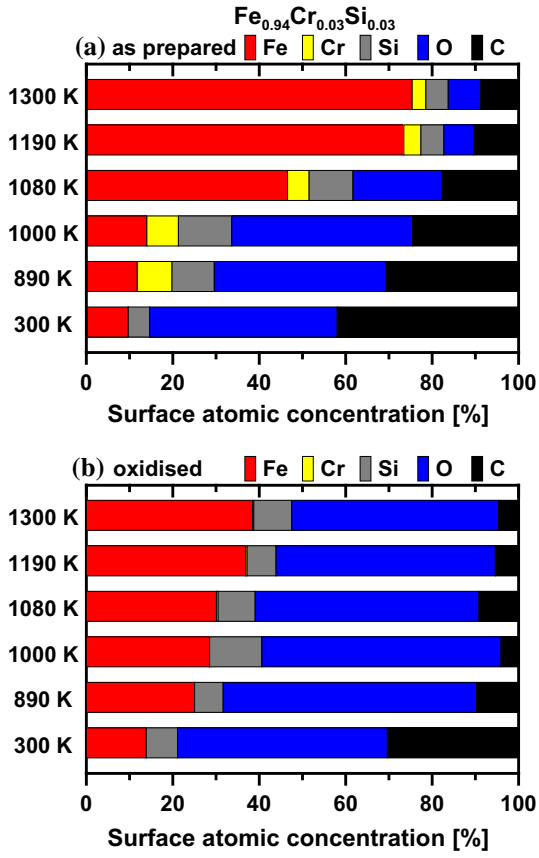

Fig. 1—(Color online) The surface atomic concentrations of selected elements for the as-prepared (*a*) and oxidized (*b*) $Fe_{0.94}Cr_{0.03}Si_{0.03}$ samples after annealing at various temperatures.

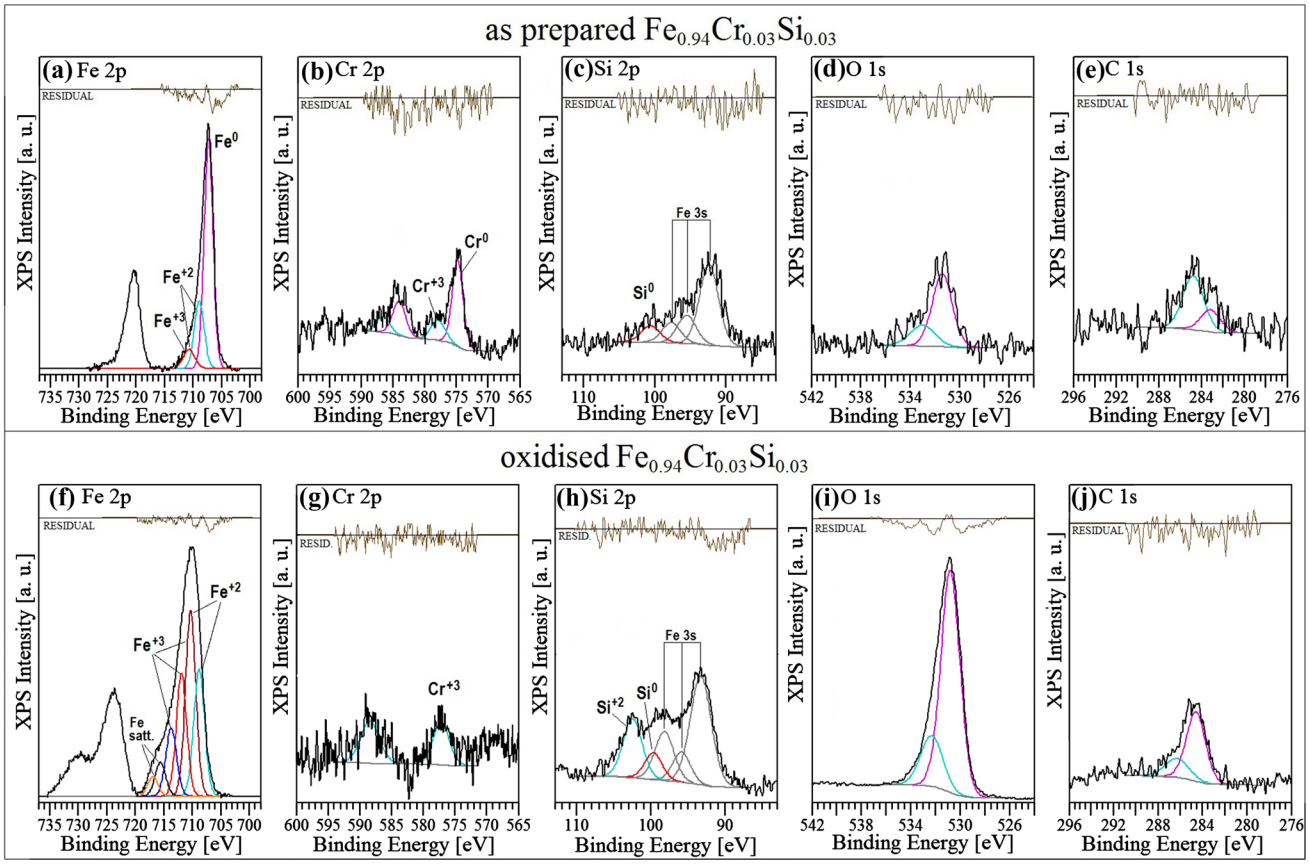

Fig. 2—(Color online) The selected XPS spectra (Fe 2p, Cr 2p, Si 2p, O 1s, and C 1s) for $Fe_{0.94}Cr_{0.03}Si_{0.03}$ alloys: (*a*) to (*e*) the as-prepared sample after annealing in UHV at 1300 K; (*f*) to (*j*) the oxidized sample after annealing in UHV at 1300 K.

In the case of the as-prepared sample, the measurements performed just after inserting into the vacuum chamber reveal that the surface is heavily contaminated by O and C atoms (see Figure 1(a)—300 K). This result is quite obvious and reflects the fact that the sample before the measurements had a direct contact with air. The determined total concentration of O and C atoms is 85.4 pct, while the concentrations of Fe, Si, and Cr are 9.7, 4.9, and 0 pct (Cr 2p XPS spectrum is not detected), respectively.

After annealing the as-prepared sample at higher temperatures, the oxygen and carbon contribution decreases gradually (see Figure 1(a)). After the last annealing at 1300 K, the surface region contains about 15 pct of O and C atoms. Desorption of contaminants during the heat treatment induces increase of the Fe content which grows systematically from 9.7 pct (RT) to 75 pct (1280 K). At the same time, changes of the Cr and Si contents are more complicated. Initially, at low temperatures, the concentration of both solutes increases, while at 1080 K and above, it decreases. That interesting result will be discussed in a later section in more detail. Nevertheless, it should be noted that the estimated c_{Si}/c_{Fe} and c_{Cr}/c_{Fe} ratios are higher (except c_{Cr}/c_{Fe} for 300 K) than the corresponding ratios calculated from the sample bulk chemical composition ($c_{Si}/c_{Fe}^{bulk} = c_{Cr}/c_{Fe}^{bulk} = 3/96 \approx 0.03$). It means that the annealing of the as-prepared sample up to 1000 K causes the segregation process of Cr and Si atoms to the surface.

Detailed analysis of XPS spectra measured for the as-prepared $Fe_{0.94}Cr_{0.03}Si_{0.03}$ sample after annealing at 1300 K (Figures 2(a) to (e)) allows to determine the oxidation state and the chemical composition of the surface region. The Fe 2p core-level line consists of three components, which are presented for the $Fe2p_{3/2}$ peak (Figure 2(a)). The main at the binding energy (BE) of 707.3 eV represents the metallic iron (Fe^0),[11,23] while the next two at the BE of 708.9 and 710.7 eV correspond to Fe^{2+} and Fe^{3+} species.[11, 23] The Cr 2p doublet (Figure 2(b)) consists of two components. The first (and dominant) is the metallic chromium (Cr^0) with the BE of 574.8 eV for $2p_{3/2}$ peak and 584.0 eV for $2p_{1/2}$ peak, while the second representing Cr^{+3} is placed at the positions of 577.9 eV ($2p_{3/2}$) and 586.6 eV ($2p_{1/2}$).[10, 24] In the case of Si 2p spectrum (Figure 2(c)), it should be pointed out that in this energy range the Fe 3s envelope occurs too, and thus the detailed deconvolution of this spectrum is necessary to obtain a reliable information about the Si 2p envelope. Proceeding in the same way as in Reference 15, the peak at the position of 99.9 eV could be assigned to Si^0 species.[15, 25] The O 1s spectrum (Figure 2(d)) exhibits small peak (comparing to the background level) which can be divided into two components: the first one at the BE of 531.4 eV and the second one at 533.0 eV.[26] The C 1s signal

(Figure 2(e)) is also weak. However, its asymmetric shape suggests the presence of two components at 283.2 and 284.8 eV.

The results obtained for the oxidized $Fe_{0.94}Cr_{0.03}Si_{0.03}$ alloy (Figure 1(b)) allow to state that the measured surface region is permanently oxidized, even after annealing at very high temperatures. The initial chemical composition of surface region is quite similar to the as-prepared one. However, during annealing only a significant decrease of carbon content is observed (from 30.4 to 4.6 pct). During thermal treatment, the oxygen contribution first increases (from 48.5 to 58.6 pct at 890 K) and then continuously decreases to 47.9 pct. The concentrations of Fe, Cr, and Si atoms gradually increase; nevertheless, the XPS signal from chromium could be observed only in the spectra measured for the sample annealed at temperatures higher than 990 K. Moreover, c_{Cr} is always lower than 0.4 pct and the c_{Cr}/c_{Fe} ratio is about 0.01. Taking into account that $c_{Cr}/c_{Fe}^{bulk} \approx 0.03$, it is clearly seen that the diffusion of Cr atoms in the oxidized sample differs from the as-prepared one. At the same time, the silicon atoms segregate from the bulk to the surface region during annealing: at 300 K the Si concentration is about 7 pct, after annealing at 1000 K it reaches 12.1 pct ($c_{Si}/c_{Fe} = 0.42$), and after annealing at 1300 K it decreases to 8.8 pct ($c_{Si}/c_{Fe} = 0.23$).

The presented XPS spectra for oxidized $Fe_{0.94}Cr_{0.03}Si_{0.03}$ alloy after annealing at 1300 K (see Figures 2(f) to (j)) exhibit broadened peak and shifted to a higher binding energy peak. Fe 2p core-level line (Figure 2(f)) is deconvoluted into six components (marked for $Fe2p_{3/2}$ peak) with the BE in the range of 708.8 to 716.9 eV, and all these energies correspond to Fe^{2+} and Fe^{3+} species.[11, 23] The chromium signal (Figure 2(g)) is at the background level; however, the 2p doublet maxima can be distinguished at the positions around 577.2 eV ($2p_{3/2}$) and 588.3 eV ($2p_{1/2}$), which represent Cr^{3+} species.[14, 26] The Si 2p spectrum is composed of two peaks (Figure 2(h)). The main is at the BE of 102.5 eV and corresponds to Fe_2SiO_4 (fayalite).[6, 15] The second at the BE of 99.7 eV represents Si^0 species—the only non-oxidized component. O 1s signal is dominant in the full binding energy range of XPS measurement and consists of two components with maxima at the position of 530.8 and 532.3 eV (Figure 2(i)). The C 1s peak intensity is close to the background; however, two components can be distinguished at the position of 284.6 and 286.3 eV (Figure 2(j)).

B. *$Fe_{0.90}Cr_{0.05}Si_{0.05}$ Alloy*

Figure 3 presents the surface atomic concentration of selected elements estimated for the as-prepared and oxidized $Fe_{0.90}Cr_{0.05}Si_{0.05}$ samples after annealing at various temperatures.

The results for as-prepared sample (see. Figure 3(a)) just after inserting into the vacuum chamber are similar to the $Fe_{0.94}Cr_{0.03}Si_{0.03}$ alloy. The estimated surface chemical composition shows that the surface region is heavily contaminated by oxygen and carbon atoms. The total contribution of these two elements is higher than

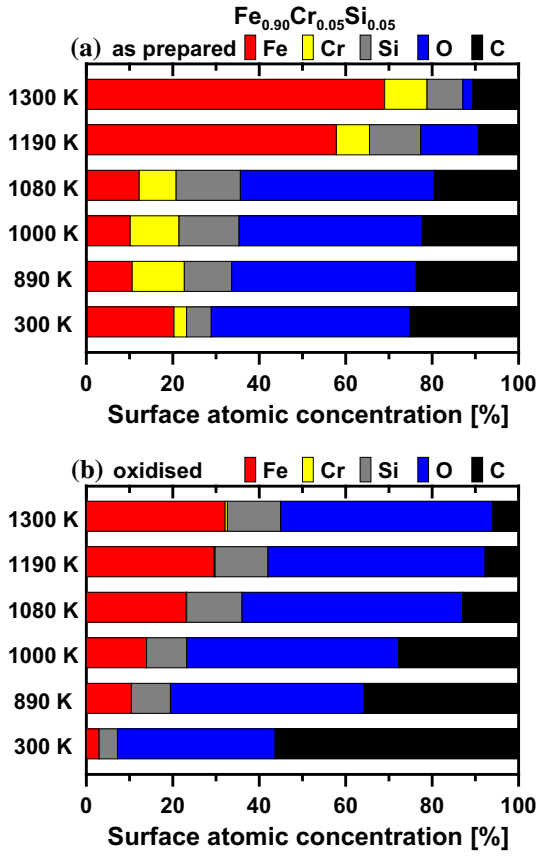

Fig. 3—(Color online) The surface atomic concentrations of selected elements for the as-prepared (*a*) and oxidized (*b*) $Fe_{0.90}Cr_{0.05}Si_{0.05}$ samples after annealing at various temperatures.

70 pct. The estimated concentrations of other elements are Fe—20.3 pct, Si—5.7 pct, Cr—3.0 pct. Annealing the sample at 890 K causes the decrease in Fe contribution to 10.6 pct and increase of Si and Cr contribution to 12.0 and 10.9 pct, respectively. Subsequent annealing induces further silicon atoms segregation, while chromium and iron concentrations decrease. Finally, after annealing at 1190 K and 1300 K, most oxygen and carbon contamination desorbs and the surface region is composed of 69.0 pct Fe atoms, 9.8 pct Cr atoms, 8.3 pct Si atoms, 2.3 pct O atoms, and 10.6 pct C atoms. The c_{Si}/c_{Fe} ratio is 0.12 and the c_{Cr}/c_{Fe} ratio is 0.14 which are about two times higher than $c_{Si}/c_{Fe}^{bulk} = c_{Cr}/c_{Fe}^{bulk} \approx 0.056$. This result clearly points out that silicon and chromium segregate to the surface of $Fe_{0.90}Cr_{0.05}Si_{0.05}$ alloy.

The initial surface chemical composition of oxidized $Fe_{0.90}Cr_{0.05}Si_{0.05}$ alloy is 92.8 pct for O and C, 3.0 pct for Fe, 4.2 pct for Si, and 0.0 pct for Cr (see Figure 3(b)). Similarly to the $Fe_{0.94}Cr_{0.03}Si_{0.03}$ sample, a weak chromium signal is detected only in the spectra measured for the sample annealed at temperatures higher than 890 K. Moreover, for the oxidized sample, oxygen is the major component of the surface region and its concentration does not change during annealing. At the same time, a significant decrease of carbon content is observed. After annealing at 1300 K, the surface is

composed of 32.1 pct Fe atoms, 0.5 pct Cr atoms, 12.3 pct Si atoms, 49.0 pct O atoms, and 6.1 pct C atoms, which means that the silicon atoms strongly segregate from the bulk to the surface, while the chromium atoms probably diffuse into deeper regions (c_{Si}/c_{Fe} ratio is 0.38 and c_{Cr}/c_{Fe} ratio is 0.02).

Figure 4 presents selected XPS spectra with detailed deconvolution after final annealing of the as-prepared and oxidized $Fe_{0.90}Cr_{0.05}Si_{0.05}$ alloys.

In the case of the as-prepared $Fe_{0.90}Cr_{0.05}Si_{0.05}$ alloy (see Figures 4(a) to (e)), after annealing at 1300 K, in the Fe 2p spectrum four components are distinguished (marked for the $Fe2p_{3/2}$ peak). The main component at the BE of 707.2 eV represents the metallic iron (Fe^0),[23] while the next three at the positions of 708.6, 710.1, and 711.8 eV correspond to Fe^{2+} and Fe^{3+} species (see Figure 4(a)).[23] The Cr 2p doublet (Figure 4(b)) is composed of two peaks representing Cr^0 species (at the BE of 574.8 eV for $2p_{3/2}$) and Cr^{3+} species (at the BE of 576.7 eV for $2p_{3/2}$).[10, 26] In the case of Si 2p spectrum (Figure 4(c)), after separation of the Fe 3s signal, the Si^0 component is distinguished at the position of 99.9 eV.[15, 25] Despite that oxygen and carbon signals are close to the background level, they are presented and analyzed. Similar to the $Fe_{0.94}Cr_{0.03}Si_{0.03}$ alloy, two components for each spectrum are distinguished: 531.8 and 533.2 eV for the O 1s (Figure 4(d)), and 283.7 and 285.6 eV for the C 1s (Figure 4(e)).[10, 15]

Results presented for the oxidized $Fe_{0.90}Cr_{0.05}Si_{0.05}$ alloy after annealing at 1300 K (Figure 4) are similar to those obtained for the oxidized $Fe_{0.94}Cr_{0.03}Si_{0.03}$ alloy. Deconvolution of Fe 2p and Cr 2p spectra exhibits peaks only at the positions corresponding to oxide compounds. In the case of the Fe 2p core-level line (Figure 4(f)), there are five peaks with the BE in the range of 709.4 to 716.8 eV (Fe^{2+} and Fe^{3+} species). The chromium signal (Figure 4(g)) is at the background level; however, the 2p doublet (correspond to Cr^{3+} species) can be distinguished with the maximum at the position around 577.6 eV ($2p_{3/2}$) and 587.3 eV ($2p_{1/2}$). In the case of the Si 2p peak (Figure 4(h)), a well-distinguished component is placed at the BE of 102.5 eV which corresponds to Fe_2SiO_4 (fayalite). However, at the BE of 99.5 eV there is a component which probably represents both Si^0 and Fe^{3+} species (from the Fe 3s envelope).[15] As it was mentioned before, the main surface component in measured surface region is oxygen. The presented O 1s envelope (Figure 4(i)) contains two components, first at the position of 531.1 eV and second at the BE of 532.5 eV. The C 1s spectrum (Figure 4(j)) is composed of two components (BE of 284.6 and 286.3 eV).

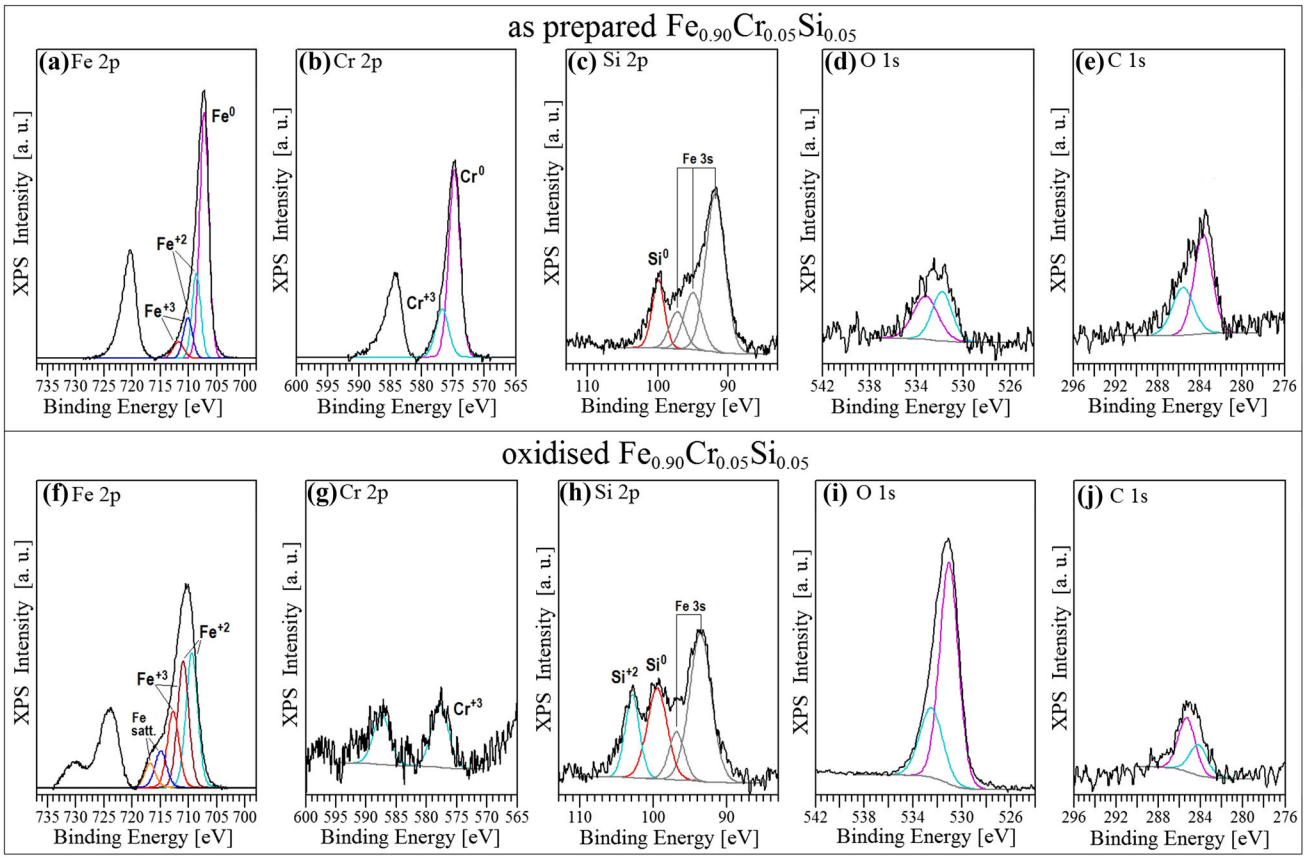

Fig. 4—(Color online) The selected XPS spectra (Fe 2p, Cr 2p, Si 2p, O 1s, and C 1s) for $Fe_{0.90}Cr_{0.05}Si_{0.05}$ alloys: (*a*) to (*e*) the as-prepared sample after annealing in UHV at 1300 K; (*f*) to (*j*) the oxidized sample after annealing in UHV at 1300 K.

C. $Fe_{0.85}Cr_{0.10}Si_{0.05}$ Alloy

Figure 5 presents the surface atomic concentration of selected elements estimated for the as-prepared and oxidized $Fe_{0.85}Cr_{0.10}Si_{0.05}$ samples after annealing at various temperatures.

At RT, in the surface region of the as-prepared $Fe_{0.85}Cr_{0.10}Si_{0.05}$ sample, the initial contributions of iron, chromium, and silicon are 16.5, 7.8, and 6.0 pct, respectively, while the total concentration of oxygen and carbon is about 69.7 pct (Figure 5(a)—300 K). The initial c_{Si}/c_{Fe} ratio is 0.36 ($c_{Si}/c_{Fe}^{bulk} \approx 0.06$) and c_{Cr}/c_{Fe} ratio is 0.47 ($c_{Cr}/c_{Fe}^{bulk} \approx 0.12$). This result implies that during the sample preparation procedure, the surface segregation process already occurred. Annealing the sample leads to changes in the chemical composition (Figure 5(a)), which are similar to those observed for the $Fe_{0.90}Cr_{0.05}Si_{0.05}$ alloys. After the last annealing at 1300 K, the surface is composed of 69.3 pct of iron, 14.4 pct of chromium and 9.2 pct of silicon, while the total concentration of oxygen and carbon is reduced to 7.1 pct. The c_{Si}/c_{Fe} ratio is 0.13 and c_{Cr}/c_{Fe} ratio is 0.21. Similar to $Fe_{0.94}Cr_{0.03}Si_{0.03}$ and $Fe_{0.90}Cr_{0.05}Si_{0.05}$ alloys, these two ratios are about two times higher than corresponding c_{Si}/c_{Fe}^{bulk} and c_{Cr}/c_{Fe}^{bulk}.

Results obtained for oxidized $Fe_{0.85}Cr_{0.10}Si_{0.05}$ alloy (Figure 5(b)) before and after annealing also imply the occurrence of segregation of silicon and chromium

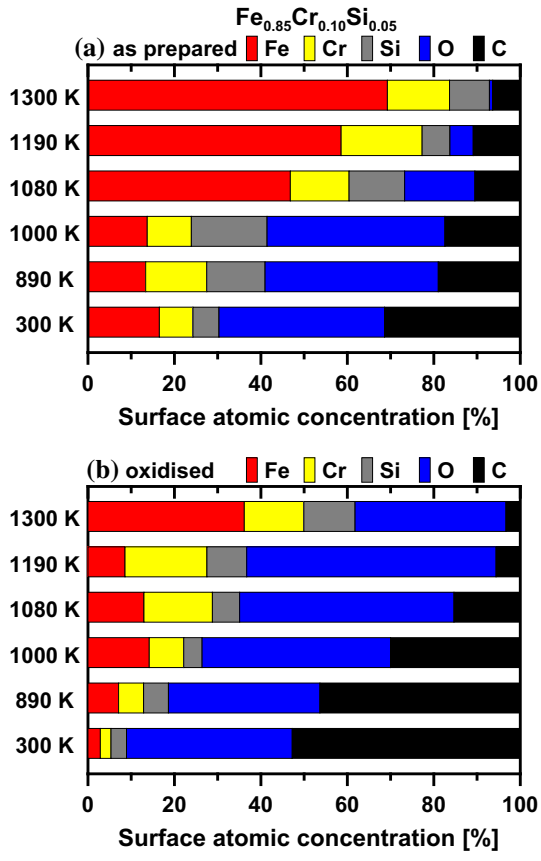

Fig. 5—(Color online) The surface atomic concentrations of selected elements for the as-prepared (*a*) and oxidized (*b*) $Fe_{0.85}Cr_{0.10}Si_{0.05}$ samples after annealing at various temperatures.

atoms. In this case, despite heavy surface contamination (91.1 pct), Fe, Si, and Cr signals are observed already at room temperature. The initial iron contribution is 2.9 pct and it consistently increases to 13.0 pct after annealing at 890 K. After annealing at higher temperatures, it gradually decreases to 8.6 pct (1190 K) and finally after heating at 1300 K it reaches 36.2 pct. The initial silicon concentration is 3.6 pct. It increases after first annealing to 5.8 pct and then drops after heating at 980 K to 4.3 pct. Further annealing causes the increase of the Si contribution—finally it reaches 11.8 pct. In the case of carbon and oxygen concentration, after annealing at 1300 K in the sample surface region 34.9 pct of O atoms and 3.3 pct of C atoms are detected. The most important difference between the oxidized $Fe_{0.85}Cr_{0.10}Si_{0.05}$ sample and the oxidized alloys with the lower content of solutes is connected with the concentration of chromium atoms. In contrast to the oxidized $Fe_{0.94}Cr_{0.03}Si_{0.03}$ and $Fe_{0.90}Cr_{0.05}Si_{0.05}$ alloys where the Cr signal was at the background level, in the oxidized $Fe_{0.85}Cr_{0.10}Si_{0.05}$ sample the initial chromium concentration is 2.5 pct. After annealing at high temperatures, the Cr content increases reaching 19.0 pct at 1180 K and 13.8 pct at 1300 K. The c_{Si}/c_{Fe} ratio is 0.33 and c_{Cr}/c_{Fe} ratio is 0.38, which are, respectively, five and three times higher than corresponding c_{Si}/c_{Fe}^{bulk} and c_{Cr}/c_{Fe}^{bulk} ratios. According to that it can be state that segregation of Cr and Si to the surface region of $Fe_{0.85}Cr_{0.10}Si_{0.05}$ alloy occurs not only during sample preparation but also during heating.

Figure 6 presents selected XPS spectra for the as-prepared and oxidized $Fe_{0.85}Cr_{0.10}Si_{0.05}$ samples after annealing in UHV at 1300 K.

The spectra for the as-prepared $Fe_{0.85}Cr_{0.10}Si_{0.05}$ sample present peaks/components similar to the alloys described before ($Fe_{0.94}Cr_{0.03}Si_{0.03}$ and $Fe_{0.90}Cr_{0.05}Si_{0.05}$). The Fe 2p doublet (Figure 6(a)) is composed of four components, from which the most dominant is the Fe^0 doublet at BE of 707.3 eV (Fe $2p_{3/2}$) and 720.4 eV (Fe $2p_{1/2}$). The Cr 2p doublet (Figure 6(b)) is deconvoluted into two components: the first at positions of 574.8 eV (Cr $2p_{3/2}$) and 584.1 eV (Cr $2p_{1/2}$) corresponds to Cr^0 and the second with maxima placed at 576.7 and 586.0 eV represents Cr^{3+} species. The Si 2p peak (Figure 6(c)) is at the BE of 100.0 eV (Si^0). The signal from O is close to the background level and due to that the position of maximum of the O 1s peak cannot be determined (Figure 6(d)). In the C 1s spectrum (Figure 6(e)), two components with BE of 283.6 and 285.9 eV are distinguished.

The results obtained for the oxidized $Fe_{0.85}Cr_{0.10}Si_{0.05}$ sample reveal that after annealing at 1300 K the surface is composed not only of Fe, Cr, and Si oxides. Signals from pure elements are also detected. The Fe 2p spectrum (Figure 6(f)) consists of four components. The main, placed at the position of 707.3 eV, corresponds to the Fe^0 species, and the rest (at the BE of 708.8, 710.6, 712.3 eV) represent Fe^{2+} and Fe^{3+} species. A line shape of chromium signal is different from those presented before for the oxidized $Fe_{0.94}Cr_{0.03}Si_{0.03}$ and $Fe_{0.90}Cr_{0.05}Si_{0.05}$ alloys. The detailed deconvolution of

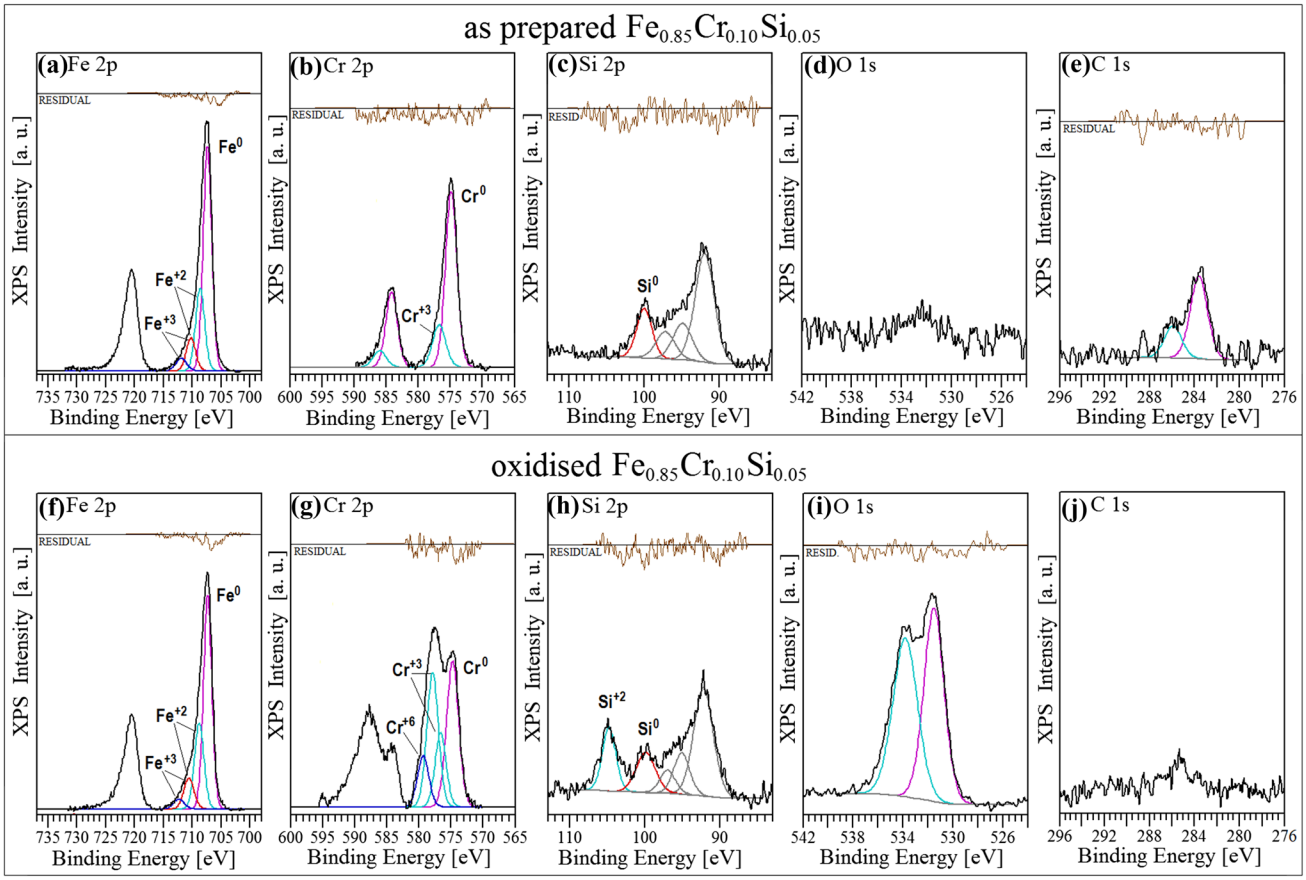

Fig. 6—(Color online) The selected XPS spectra (Fe 2p, Cr 2p, Si 2p, O 1s, and C 1s) for $Fe_{0.85}Cr_{0.10}Si_{0.05}$ alloys: (*a*) to (*e*) the as-prepared sample after annealing in UHV at 1300 K; (*f*) to (*j*) the oxidized sample after annealing in UHV at 1300 K.

Cr $2p_{3/2}$ peak (Figure 6(g)) reveals four components. The first, placed at the lowest BE of 574.7 eV, is related to the Cr^0, the next two at BE of 576.6 and 577.8 eV correspond to Cr^{3+}, and the last one, which is the maximum placed at 579.3 eV, represents Cr^{6+}.[14, 26] In the case of the Si 2p spectrum (Figure 6(h)), two components at BE of 99.9 and 104.8 eV, related to Si^0 and Si^{4+} (SiO_2), are distinguished. Here, it is worth noting that the signal from SiO_2 appears for the first time in this work. All Si 2p spectra, analyzed before, contains only components connected with Si^0 or/and Fe_2SiO_4 (fayalite). In the O 1s spectrum, two local maxima are visible. This indicates the presence at least of two peaks (at BE of 531.5 and 533.8 eV). The position of maximum of the C 1s peak (Figure 6(j)) cannot be determined due to the low signal/background intensity ratio.

D. *$Fe_{0.80}Cr_{0.15}Si_{0.05}$ Alloy*

Figure 7 presents the surface atomic concentration for the as-prepared and oxidized $Fe_{0.80}Cr_{0.15}Si_{0.05}$ alloys after annealing at various temperatures. Figure 8 presents the selected XPS spectra for the same samples after annealing in UHV at 1300 K.

In the case of the as-prepared sample (Figure 7(a)), the measurements performed at RT and after subsequent annealing up to 1300 K present a standard cleaning process of C and O contaminations and the surface segregation of Cr and Si solutes. The changes of carbon and oxygen concentrations during sample annealing are similar to those observed previously for all the as-prepared samples. After annealing at 1300 K, the contribution of C atoms is 4.6 pct, while the O contribution is 2.3 pct. The Fe contribution consequently increases from 9.2 pct (RT) to 61.7 pct (for 1300 K). The surface atomic concentration of chromium for the sample at RT is 7.8 pct, after annealing at 890 K it is over twice higher, but after annealing at 1000 K it decreases to 15.1 pct. Further sample heating causes increase in the Cr contribution up to 25.0 pct. Finally, after annealing at 1300 K, the Cr contribution is 23.8 pct. The silicon concentration firstly increases from 2.9 to 12.4 pct and 16.2 pct after annealing at 890 K and 1000 K, respectively. Further heating at higher temperatures causes decrease inthe Si content, which reaches 7.6 pct after last annealing at 1300 K. The final c_{Si}/c_{Fe} and c_{Cr}/c_{Fe} ratios are 0.12 and 0.39, respectively. Similar to other as-obtained alloys, these two ratios are about two times higher than $c_{Si}/c_{Fe}^{bulk} \approx 0.06$ and $c_{Cr}/c_{Fe}^{bulk} \approx 0.19$.

The selected XPS spectra for the as-prepared $Fe_{0.80}Cr_{0.15}Si_{0.05}$ alloy after annealing at 1300 K (Figures 8(a) to (e)) show the Fe 2p core-level line

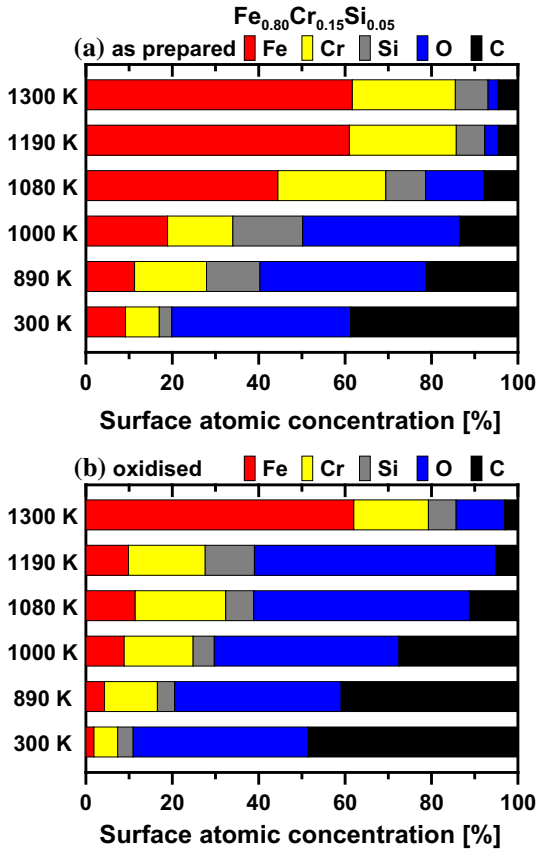

Fig. 7—(Color online) The surface atomic concentrations of selected elements for the as-prepared (*a*) and oxidized (*b*) $Fe_{0.80}Cr_{0.15}Si_{0.05}$ samples after annealing at various temperatures.

which is composed of three peaks (Figure 8(a)). The main one, marked for $Fe2p_{3/2}$, is Fe^0 at the BE of 707.3 eV, while the peaks at the BE of 708.9 and 710.8 eV correspond to Fe^{2+} and Fe^{3+} species. The Cr 2p doublet (Figure 8(b)) exhibits two components at the positions of 574.7 and 576.5 eV (for $2p_{3/2}$) which represent Cr^0 and Cr^{3+} species. The analysis of the Si 2p spectrum (Figure 8(c)) allows to distinguish a dominant Si^0 species (BE of 99.9 eV) and additional peak which probably represents a non-stoichiometric Si-O_x bond (BE of 101.5 eV).[15] The O 1s spectrum (Figure 8(d)) is composed of two peaks at the BE of 530.8 and 531.9 eV, while C 1s signal (Figure 8(e)) exhibits three components at the position of 283.5, 284.8, and 286.3 eV.

The XPS measurements performed for the oxidized $Fe_{0.80}Cr_{0.15}Si_{0.05}$ alloy reveal that the iron, chromium, and silicon concentrations consequently increase during sample annealing up to 1080 K. At this stage, the estimated surface atomic concentrations are Fe—11.4 pct, Cr—21.0 pct, Si—6.5 pct, O—49.9 pct, C—11.2 pct (see Figure 7(b)–1080 K). Further annealing at 1190 K causes the decrease of Fe, Cr, and C contributions and increase of Si and O content. Finally, after annealing the sample at 1300 K, the studied surface region is composed of 62 pct of Fe atoms, 12.3 pct of Cr atoms, 6.4 pct of Si atoms, and only 11.3 pct of O atoms and 3.0 pct of C atoms (see Figure 7(b)-1300 K). High chromium concentration observed during all stages of thermal treatment indicates segregation of Cr to the surface region of the oxidized $Fe_{0.80}Cr_{0.15}Si_{0.05}$ alloy. In addition, after annealing at 1300 K, the oxygen content significantly decreases. In the case of the studied oxidized samples that effect is observed for the first time. It may suggest that the higher concentration of Si and Cr in this alloy indicates the formation of thinner passivation layer during the sample oxidation process. It will be discussed in a later section in more detail.

The results obtained for the final state of oxidized $Fe_{0.80}Cr_{0.15}Si_{0.05}$ alloy (after annealing at 1300 K) are presented at Figures 8(f) to (j). The Fe 2p core-level line (Figure 8(f)) is quite similar to the $Fe_{0.85}Cr_{0.10}Si_{0.05}$ alloy. The $2p_{3/2}$ peak exhibits three components, from which the dominant one represents Fe^0 species at the BE of 707.3 eV, while the other two (at BE of 708.7 and 710.8 eV) correspond to Fe^{2+} and Fe^{3+} species. A line shape of Cr 2p spectrum is close to this observed for the as-prepared sample (see Figures 8(g) and (b)). Three components are distinguished in the Cr $2p_{3/2}$ peak: 574.6, 576.2, and 577.8 eV, which correspond to Cr^0 and Cr^{3+} species. In the case of the Si 2p spectrum, only Si^0 peak is observed at the BE of 99.8 eV (Figure 8(h)). The O 1s core-level line is composed of two peaks with maxima at the positions of 531.7 and 533.8 eV (Figure 8(i)), while the maximum of C 1s signal is around 284.7 eV (the exact position cannot be identified due to the low signal/background intensity ratio, see Figure 8(j)).

IV. DISCUSSION

As it was described above, all studied samples were prepared in the same way and then were subjected to the similar regime of thermal treatment in UHV. Firstly, it should be noted that the behavior of the adsorbed C atoms is similar for all studied as-obtained and oxidized Fe-Cr-Si alloys. The C contamination which is mainly connected with the direct contact of the studied samples with air during preparation procedure tends to systematically decrease with samples annealing in UHV. In addition, the detailed analysis of all XPS C 1s signals as well as results reported in Reference 27 showed that the adsorbed carbon atoms do not form any compounds with Fe, Cr, and Si in the studied Fe-Cr-Si alloys. Therefore, it seems that the influence of C atoms on the surface segregation process as well as corrosion of the studied alloys is negligibly small and due to that it will not be discussed further.

In general, it can be stated that the obtained results for all as-prepared samples are quite similar to each other. In the case of the oxidized samples, the applied thermal treatment allows to obtain different surface chemical compositions, which are probably directly related to the initial bulk concentration of both solutes. Taking this into account, the following discussion is divided into three separate parts.

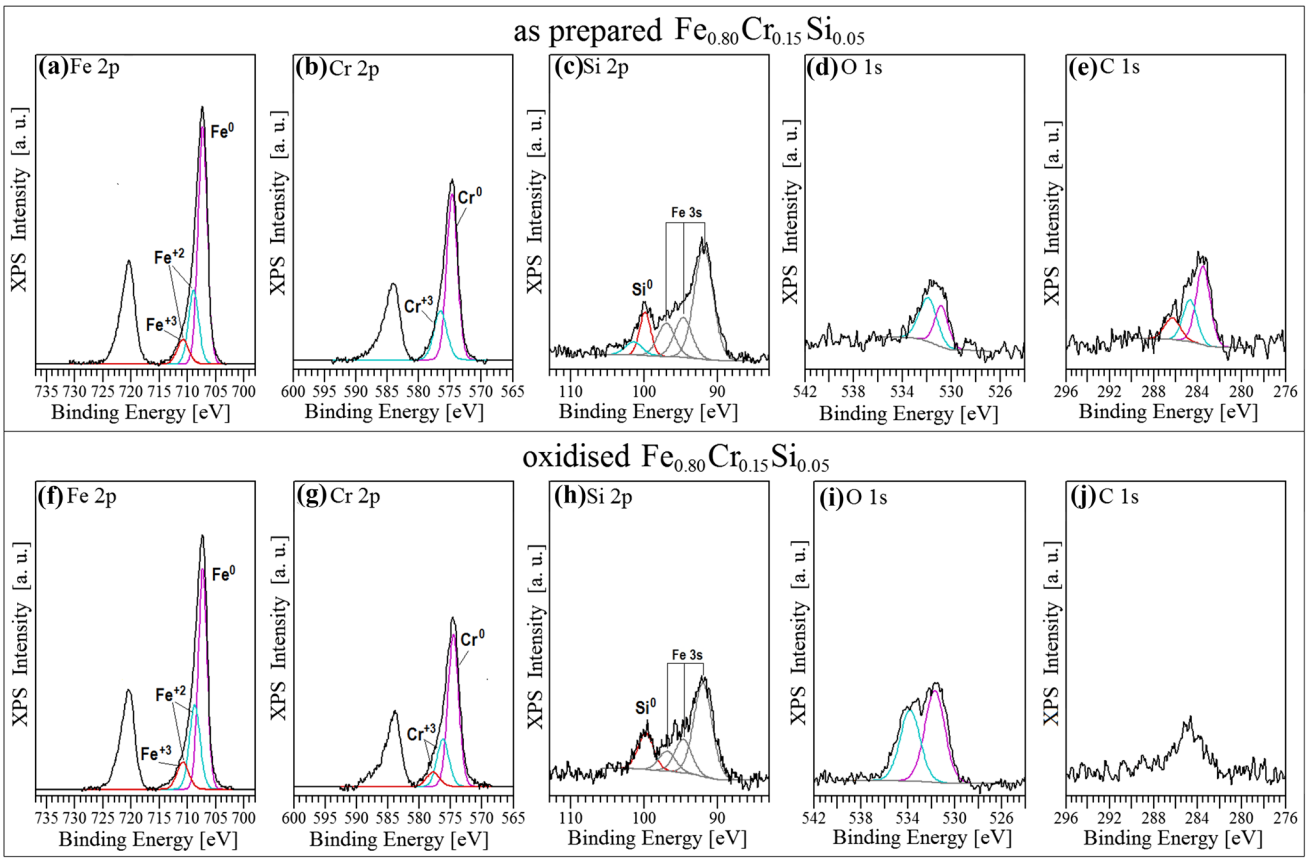

Fig. 8—(Color online) The selected XPS spectra (Fe 2p, Cr 2p, Si 2p, O 1s) for $Fe_{0.80}Cr_{0.15}Si_{0.05}$ alloys: (*a*) to (*e*) the as-prepared sample after annealing in UHV at 1300 K; (*f*) to (*j*) the oxidized sample after annealing in UHV at 1300 K.

Table I. Calculated c_{Si}/c_{Fe} and c_{Cr}/c_{Fe} Ratios for the As-Prepared Samples

	$Fe_{0.94}Cr_{0.03}Si_{0.03}$		$Fe_{0.90}Cr_{0.05}Si_{0.05}$		$Fe_{0.85}Cr_{0.10}Si_{0.05}$		$Fe_{0.80}Cr_{0.15}Si_{0.05}$	
T [K]	c_{Si}/c_{Fe}	c_{Cr}/c_{Fe}	c_{Si}/c_{Fe}	c_{Cr}/c_{Fe}	c_{Si}/c_{Fe}	c_{Cr}/c_{Fe}	c_{Si}/c_{Fe}	c_{Cr}/c_{Fe}
RT	0.51	0.00	0.38	0.15	0.36	0.47	0.32	0.85
890	0.83	0.68	1.03	1.13	1.01	1.06	1.10	1.48
1000	0.88	0.52	1.27	1.11	1.28	0.74	0.85	0.80
1080	0.22	0.11	1.21	0.70	0.27	0.29	0.21	0.56
1190	0.07	0.05	0.20	0.13	0.11	0.32	0.11	0.41
1300	0.07	0.04	0.12	0.14	0.13	0.21	0.12	0.39
Bulk Ratio	0.032	0.032	0.056	0.056	0.059	0.118	0.063	0.188

A. *As-Prepared Samples*

Table I presents c_{Si}/c_{Fe} and c_{Cr}/c_{Fe} ratios for all as-prepared samples calculated according to Eq. 1. Despite the different bulk chemical composition of the studied alloys, the "diffusion behavior" of both solutes is quite similar for all samples. The much higher initial c_{Si}/c_{Fe} and c_{Cr}/c_{Fe} ratios than the corresponding c_{Si}/c_{Fe}^{bulk} and c_{Cr}/c_{Fe}^{bulk} ones indicate the strong surface segregation process of Si and Cr atoms during the samples preparation procedure. After the first annealing at 890 K, the c_{Si}/c_{Fe} and c_{Cr}/c_{Fe} ratios increase significantly (in most cases, the obtained values are more than ten times higher than the corresponding bulk ratios). This means that despite the occurrence of solutes segregation during the sample preparation, the thermal treatment at UHV enhances this process. Annealing at 1000 K results in further increase of c_{Si}/c_{Fe} values but c_{Cr}/c_{Fe} ratios start to decrease. Above 1000 K, a gradual decrease of both solute:iron ratios are observed. However, even after annealing at the highest temperature the surface c_{Si}/c_{Fe} and c_{Cr}/c_{Fe} ratios are still about two times higher than the bulk ones. The comparison of the values presented in Table I with the oxygen surface concentrations

estimated for all as-prepared samples (Figures 1(a), 3(a), 5(a), 7(a)) indicates that the surface segregation process is strongly correlated with the presence of the oxygen atoms on the surface. As one can notice, up to 1000 K there are significant amounts of oxygen atoms at the alloy surfaces (41.9 pct for $Fe_{0.94}Cr_{0.03}Si_{0.03}$, 42.2 pct for $Fe_{0.90}Cr_{0.05}Si_{0.05}$, 41.1 pct for $Fe_{0.85}Cr_{0.10}Si_{0.05}$, and 36.3 pct for $Fe_{0.80}Cr_{0.15}Si_{0.05}$), while annealing at 1080 K induces rapid decrease of the oxygen contribution in the surface region.

According to the presented results, the evolution of the surface chemical composition of all as-prepared samples could be described as below. After melting and cold-rolling processes, the Fe-Cr-Si alloys foils were annealed in vacuum at 1270 K. According to the work of Idczak *et al.*,[11] the "freezing" temperature for iron-based alloys which is defined as the upper limit of temperatures at which the diffusion of atoms in the material practically does not exist is about 700 K. Taking this fact into account, it could be stated that during heating at temperatures above 700 K the Si and Cr atoms segregate to the surface region. After preparation, the samples were mounted in the UHV chamber and subsequently annealed. As it was shown above, after the first annealing in UHV, the c_{Si}/c_{Fe} and c_{Cr}/c_{Fe} ratios increase rapidly. This effect could be explained by assuming the oxygen induced surface segregation of Si and Cr atoms. The initial presence of oxygen atoms at the alloy surface (as a contaminant) probably leads to additional surface segregation of Si and Cr atoms at temperatures above 700 K. This phenomenon was observed many times in the case of iron-based alloys.[28,29]

On the basis of the results presented in Table I, it can be noticed that the maximum of c_{Si}/c_{Fe} ratio for all measured as-prepared alloys are obtained after annealing at 1000 K, while the maximum of c_{Cr}/c_{Fe} ratio is after heating at 890 K. It means that the sublimation of Cr oxides at elevated temperatures at a rate is faster than Si oxides. Further annealing at 1080 K and above induces mostly desorption of O atoms and also some amount of Fe, Cr, and Si oxides. Oxygen depletion in the surface region causes a significant slowdown of the segregation process and due to that the c_{Si}/c_{Fe} and c_{Cr}/c_{Fe} ratios systematically decrease. In summary, this part of the study indicates that the surface segregation process of Si and Cr atoms occurs in all as-prepared Fe-Cr-Si alloys and, moreover, this process depends strongly on the presence of oxygen atoms at the alloy surface. The diffusion of Cr and Si atoms to the surface region is more effective when the surface contains of oxygen atoms.

B. *Oxidized $Fe_{0.94}Cr_{0.03}Si_{0.03}$ and $Fe_{0.90}Cr_{0.05}Si_{0.05}$ Samples*

Table II presents the c_{Si}/c_{Fe}, c_{Cr}/c_{Fe} and $c_O/(c_{Fe}+c_{Si}+c_{Cr})$ ratios for the oxidized $Fe_{0.94}Cr_{0.03}Si_{0.03}$ and $Fe_{0.90}Cr_{0.05}Si_{0.05}$ samples. The comparison of the estimated c_{Si}/c_{Fe} and c_{Cr}/c_{Fe} ratios at RT with the corresponding ones obtained for the as-prepared samples reveals that the exposure to air at 870 K for 2 hours causes the additional segregation of Si atoms on the surface. Especially, in the case of $Fe_{0.90}Cr_{0.05}Si_{0.05}$ alloy the initial c_{Si}/c_{Fe} ratio is more than three times higher that c_{Si}/c_{Fe} ratio for the as-prepared sample, while the c_{Cr}/c_{Fe} ratio is close to zero. It can be stated that oxidation at high temperature, higher than the "freezing" temperature, induces diffusion of Cr atoms from the surface region toward deeper sample layers. This effect is rather surprising since the surface segregation of Cr atoms occurs in the as-obtained Fe-Cr-Si samples (Table I) as well in many binary Fe-Cr alloys which were studied previously.[4, 8–10, 14] That result could be compared with the Mössbauer spectroscopy data obtained for similar systems.[16] One of the conclusions which could be drawn from the high-temperature corrosion study of Fe-Cr-Si alloys is that the addition of a relatively small amount of Cr (≤ 5 pct) to the dilute iron-based Fe-Si alloy does not improve the anti-corrosion properties of the alloy. All of that leads to the supposition that for the alloys with low bulk concentration of Cr and Si solutes, the role of Cr atoms in the high-temperature corrosion is negligibly small.

An evolution of the surface chemical composition of the oxidized $Fe_{0.94}Cr_{0.03}Si_{0.03}$ and $Fe_{0.90}Cr_{0.05}Si_{0.05}$ samples after annealing in UHV is quite obvious. The c_{Cr}/c_{Fe} ratios are still close to zero, while the c_{Si}/c_{Fe} and $c_O/(c_{Fe}+c_{Si}+c_{Cr})$ decrease systematically with increasing temperature of annealing.

A XPS analysis of selected Fe $2p_{3/2}$ and Si 2p peaks for oxidized $Fe_{0.90}Cr_{0.05}Si_{0.05}$ sample is presented in Figure 9 (the results for the $Fe_{0.94}Cr_{0.03}Si_{0.03}$ alloy are similar and thus they are not shown here). At RT, the Fe 2p core-level line is located in the binding energy range representing only iron oxides—deconvolution of Fe $2p_{3/2}$ peak exhibits three components at BE of 710.4, 711.9, and 713.7 eV.[11, 15] At the same time, the Si 2p spectrum is composed of two peaks at BE of 103.6 and 101.0 eV which correspond to SiO_2 and SiO_x.[15] After annealing at 1000 K, the chemical shifts are observed in the spectra. Iron components (corresponding to various oxides) are placed at 709.7, 711.5, and 713.5 eV, while the silicon peak is located at 103.0 eV and is related to the presence of the Fe_2SiO_4 compound.[15, 30] According to the Mössbauer data taken for the oxidized Fe-Si [15] and Fe-Cr-Si [16] alloys, the formation of this oxide was not observed. It seems that the Fe_2SiO_4 is formed during sample oxidation in the deeper sample layers. After annealing at 1000 K, the c_{Si}/c_{Fe} and $c_O/(c_{Fe}+c_{Si}+c_{Cr})$ ratios decrease by more than a half (Table II) which implies that significant amount of oxygen desorbs and the partially reduced iron and silicon oxides form additional Fe_2SiO_4 compound.[6, 30] Further annealing causes changes mostly in the Fe 2p core-level line. The line shape changes on the higher binding energy site and two additional components could be observed with BE of 714.9 and 716.8 eV which are the Fe^{2+} satellites.[11, 23] Finally, it is worth noting that all spectra presented in Figure 9 do not present the Fe^0 and Si^0 species. The comparison of this result with those obtained for the oxidized $Fe_{0.95}Si_{0.05}$ alloy,[15] where annealing at similar temperatures revealed the presence of Fe^0 and Si^0 species, indicates that the oxygen atoms diffuse easier

Table II. Calculated c_{Si}/c_{Fe}, c_{Cr}/c_{Fe} and $c_O/(c_{Fe} + c_{Si} + c_{Cr})$ Ratios for the Oxidized $Fe_{0.94}Cr_{0.03}Si_{0.03}$ and $Fe_{0.90}Cr_{0.05}Si_{0.05}$ Samples

	$Fe_{0.94}Cr_{0.03}Si_{0.03}$			$Fe_{0.90}Cr_{0.05}Si_{0.05}$		
T [K]	c_{Si}/c_{Fe}	c_{Cr}/c_{Fe}	$c_O/(c_{Fe} + c_{Si} + c_{Cr})$	c_{Si}/c_{Fe}	c_{Cr}/c_{Fe}	$c_O/(c_{Fe} + c_{Si} + c_{Cr})$
RT	0.52	0.00	2.30	1.43	0.00	5.06
890	0.26	0.00	1.85	0.86	0.00	2.30
1000	0.42	0.00	1.36	0.67	0.00	2.11
1080	0.28	0.01	1.33	0.55	0.01	1.42
1190	0.18	0.01	1.16	0.41	0.01	1.20
1300	0.23	0.01	1.01	0.38	0.02	1.09
Bulk Ratio	0.032	0.032	—	0.056	0.056	—

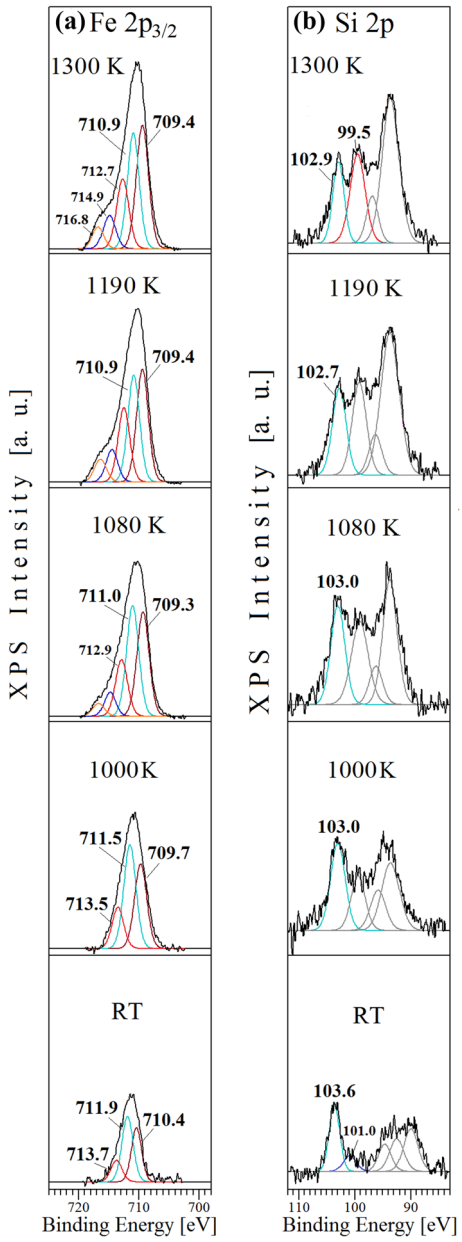

Fig. 9—(Color online) The selected XPS spectra for the $Fe_{0.90}Cr_{0.05}Si_{0.05}$ alloy after annealing at various temperatures: (*a*) Fe $2p_{3/2}$ peak, (*b*) Si 2p spectrum.

into deeper parts of the $Fe_{0.90}Cr_{0.05}Si_{0.05}$ alloy than it was observed for the $Fe_{0.95}Si_{0.05}$ one. This result confirms the observation that the addition of a relatively small amount of Cr (≤ 5 pct) to the dilute iron-based Fe-Si alloy does not improve the anti-corrosion properties of the alloy. According to this part of discussion that effect is mainly connected with the absence of Cr atoms in the surface region.

C. *Oxidized $Fe_{0.85}Cr_{0.10}Si_{0.05}$ and $Fe_{0.80}Cr_{0.15}Si_{0.05}$ Samples*

The values of c_{Si}/c_{Fe}, c_{Cr}/c_{Fe} and $c_O/(c_{Fe} + c_{Si} + c_{Cr})$ ratios presented in Table III and the detailed deconvolution of selected peaks arranged in Figure 10 (for $Fe_{0.80}Cr_{0.15}Si_{0.05}$ alloy as an example) reveal a systematic desorption of oxides caused by the thermal treatment of the oxidized $Fe_{0.85}Cr_{0.10}Si_{0.05}$ and $Fe_{0.80}Cr_{0.15}Si_{0.05}$ samples. As one can notice, the initial c_{Si}/c_{Fe} and c_{Cr}/c_{Fe} ratios are much higher than the corresponding ones for the as-prepared samples (Table I), which means that during the oxidation process both solutes additionally segregate to the surface. At the same time, comparing the initial c_{Si}/c_{Fe} and c_{Cr}/c_{Fe} ratios estimated for the oxidized $Fe_{0.90}Cr_{0.05}Si_{0.05}$ (Table II) and $Fe_{0.85}Cr_{0.10}Si_{0.05}$ (Table III) samples it can be clearly seen that increasing the bulk chromium content from 5 at. pct to 10 pct induces opposite diffusion direction of Cr atoms during the high-temperature oxidation process. Moreover, taking into account Mössbauer data which show that the high-temperature corrosion of $Fe_{0.85}Cr_{0.10}Si_{0.05}$ alloy is almost stopped at 870 K and 1070 K, while in the case of $Fe_{0.96}Cr_{0.03}Si_{0.01}$, $Fe_{0.94}Cr_{0.03}Si_{0.03}$, and $Fe_{0.90}Cr_{0.05}Si_{0.05}$ samples a rather fast corrosion rates were observed,[16] it seems that the surface passivation layer which could prevent further diffusion of oxygen into deeper regions of the Fe-Cr-Si alloy must be composed of both Si and Cr oxides.

Annealing the samples at 890 K and 1000 K causes the decrease of c_{Si}/c_{Fe}, c_{Cr}/c_{Fe} and $c_O/(c_{Fe} + c_{Si} + c_{Cr})$ ratios indicating the successive desorption of oxygen as well as various oxides from the surface. At this stage of experiment, the Cr and Si diffusion toward the alloy/oxide interface occurs. Core-level lines, describing iron, chromium, and silicon compounds, change in shapes

after annealing at 890 K and 1000 K and exhibit numerous of components (Figure 10). In the Fe $2p_{3/2}$ peak, four components are distinguished from which the metallic Fe occurs at BE of 707.3 eV and the rest, placed at 708.8, 710.1, and 711.8 eV, correspond to Fe^{2+} and Fe^{3+} species. The Cr $2p_{3/2}$ peak is divided into three components at the BE of 576.2, 577.6 (Cr^{3+}) and 579.2 eV (Cr^{6+}).[14] The Si 2p spectrum exhibits two components, from which more dominant is SiO_2 at position of 103.2 eV (shifted by 0.3 eV in comparison to maximum at RT) and Si^0 at position of 99.7 eV.[15] In contrast to results obtained for the oxidized $Fe_{0.90}Cr_{0.05}Si_{0.05}$ sample, the presence of Fe_2SiO_4 is not detected.

Annealing the samples at 1080 K and 1190 K induces increase of the c_{Si}/c_{Fe} and c_{Cr}/c_{Fe} ratios, while $c_O/(c_{Fe} + c_{Si} + c_{Cr})$ is still decreasing. It means that during these stages of thermal treatment, the further desorption of oxygen and oxides occurs. The Fe $2p_{3/2}$ spectrum is still composed of several peaks, but their relative contribution is different. The dominant one is Fe^0 with the contribution in iron signal higher than 50 pct. In the Cr $2p_{3/2}$ and Si 2p spectra, the peaks corresponding to metallic Cr (574.6 eV) and Si^0 (99.7 eV) are also observed. Comparing this with results obtained for oxidized $Fe_{0.88}Cr_{0.12}$ and $Fe_{0.85}Cr_{0.15}$ alloys in Reference 14, where after samples annealing, the metallic Fe detected was detected but a dominant species were Fe^{2+} and Fe^{3+},[14] it can be pointed out that by adding to Fe-Cr alloys, with a higher bulk chromium content, an additional Si solute, the corrosion resistivity can be improved. Moreover, detection in the XPS spectra signals from metallic Fe, Cr, and Si indicates that the thickness of the oxide layer becomes smaller than the XPS sampling depth.

After the last annealing at 1300 K, a significant decrease of the c_{Si}/c_{Fe}, c_{Cr}/c_{Fe} and $c_O/(c_{Fe} + c_{Si} + c_{Cr})$ ratios is observed. For the oxidized $Fe_{0.80}Cr_{0.15}Si_{0.05}$ alloy, $c_O/(c_{Fe} + c_{Si} + c_{Cr})$ ratio is the lowest of all oxidized samples, which means that the measured surface region is mostly composed of pure alloy elements. In addition, the detailed deconvolution of the Fe $2p_{3/2}$, Cr $2p_{3/2}$ and Si 2p spectra reveals that the Fe^0, Cr^0, and Si^0 components are dominant (Figure 10). The Fe $2p_{3/2}$ peak is composed of three peaks representing: metallic Fe^0 at BE of 707.3 eV, Fe^{2+}, and Fe^{3+} species at BE of 708.7 and 710.8 eV. In the Cr $2p_{3/2}$ core-level line, the main component becomes metallic Cr at the position of 574.6 eV, while the other two correspond to Cr^{3+}. In the Si spectrum, only Si^0 peak is distinguished at the BE of 99.8 eV. These results confirm the Mossbauer data which show that the exposure of the $Fe_{0.85}Cr_{0.10}Si_{0.05}$ alloy to air at 870 K for 2 hours causes the formation of only very thin oxide layer (less than 20 nm) and it could be easily removed from the alloy surface by the applied thermal treatment.[16]

According to the presented data, it can be stated that the anti-corrosion properties of the Fe-Cr-Si alloys strongly depend on several factors. The most important one is the segregation of both solutes to the surface during the oxidation process, which strongly depends on their initial bulk concentration. In other words, the passive film, which prevents further diffusion of oxygen atoms into deeper sample layer, must be composed of Cr and Si oxides. As in the case of binary Fe-Cr [14] and Fe-Si [15] alloys, where this condition cannot be fulfilled, the absence of Cr atoms in the surface region of the oxidized $Fe_{0.94}Cr_{0.03}Si_{0.03}$ and $Fe_{0.90}Cr_{0.05}Si_{0.05}$ alloys is mainly responsible for the relatively fast oxidation rate. At the same time, the corrosion properties of the $Fe_{0.85}Cr_{0.10}Si_{0.05}$ and $Fe_{0.80}Cr_{0.15}Si_{0.05}$ alloys are greatly enhanced since during the oxidation procedure both solutes strongly segregate to the surface.

Another important issue is the presence of the fayalite compound. The XPS data obtained for the oxidized $Fe_{0.96}Si_{0.04}$, $Fe_{0.95}Si_{0.05}$, and $Fe_{0.90}Si_{0.10}$ alloys in Reference 15 as well as the results presented in this work reveal the presence of Fe_2SiO_4 in the surface regions of $Fe_{0.94}Cr_{0.03}Si_{0.03}$ and $Fe_{0.90}Cr_{0.05}Si_{0.05}$ samples; however, in the case of $Fe_{0.85}Cr_{0.10}Si_{0.05}$ and $Fe_{0.80}Cr_{0.15}Si_{0.05}$ alloys, all measured Si 2p spectra present only the SiO_2 components (together with the Si^0 after annealing). At this time, it should be pointed out that the presence or absence of the Fe_2SiO_4 compound is not directly connected with the initial Si bulk concentration but with the presence of Cr atoms in the passivation layer (occurrence of chromium segregation to the surface region). Similar observation has been made by Moon et al. in Reference 31 who studied the initial oxidation resistance of Fe-Cr-Si alloys in 1200 °C steam, as a function of Cr concentration. They reported that $FeCr_2O_4$, Fe_2SiO_4, and islands of amorphous SiO_2 are present in the oxide layer of $Fe_{86}Cr_{12}Si_2$ and $Fe_{84}Cr_{16}Si_2$, while Cr_2O_3 and continuous amorphous SiO_2 films are observed in the oxide layer of the $Fe_{78}Cr_{20}Si_2$ alloy. They concluded that due to sufficient Cr content, the $Fe_{78}Cr_{20}Si_2$ alloy forms a Cr_2O_3 oxide layer and under the protection of the Cr_2O_3 oxide layer, Si can react with oxygen and form a continuous, amorphous SiO_2 layer. The fast formation of Cr_2O_3 plays a key role in the formation of the continuous SiO_2 layer and the resultant oxidation resistance of the Fe-Cr-Si alloys with higher Cr content.

Finally, what should be also taken into account is the oxygen induced surface segregation of solutes (both Cr and Si atoms) during annealing in UHV. As it is shown for the as-prepared samples, the initial oxidation (pre-oxidation) of the alloys, which was connected with their direct contact with air, causes additional strong segregation of both solvents during annealing them at temperatures below 1000 K.

V. CONCLUSIONS

The XPS study of the as-prepared and oxidized Fe-Cr-Si alloys greatly expands the knowledge about the surface segregation process of the Cr and Si atoms during the sample preparation and provides information about changes in chemical composition of surface regions caused by annealing the samples at various temperatures in UHV. The obtained results together with TMS and CEMS data reported previously give a clear evidence that the anti-corrosion properties of these alloys strongly depend on the initial bulk concentration

Table III. Calculated c_{Si}/c_{Fe}, c_{Cr}/c_{Fe} and $c_O/(c_{Fe} + c_{Si} + c_{Cr})$ Ratios for the Oxidized $Fe_{0.85}Cr_{0.10}Si_{0.05}$ and $Fe_{0.80}Cr_{0.15}Si_{0.05}$ Samples

	$Fe_{0.85}Cr_{0.10}Si_{0.05}$			$Fe_{0.80}Cr_{0.15}Si_{0.05}$		
T [K]	c_{Si}/c_{Fe}	c_{Cr}/c_{Fe}	$c_O/(c_{Fe} + c_{Si} + c_{Cr})$	c_{Si}/c_{Fe}	c_{Cr}/c_{Fe}	$c_O/(c_{Fe} + c_{Si} + c_{Cr})$
RT	1.26	0.86	4.30	1.92	2.95	3.71
890	0.81	0.82	1.88	0.92	2.83	1.88
1000	0.30	0.56	1.65	0.55	1.80	1.44
1080	0.49	1.22	1.41	0.57	1.84	1.29
1190	1.08	2.21	1.57	1.16	1.80	1.43
1300	0.33	0.38	0.57	0.10	0.28	0.13
Bulk Ratio	0.059	0.118	—	0.063	0.188	—

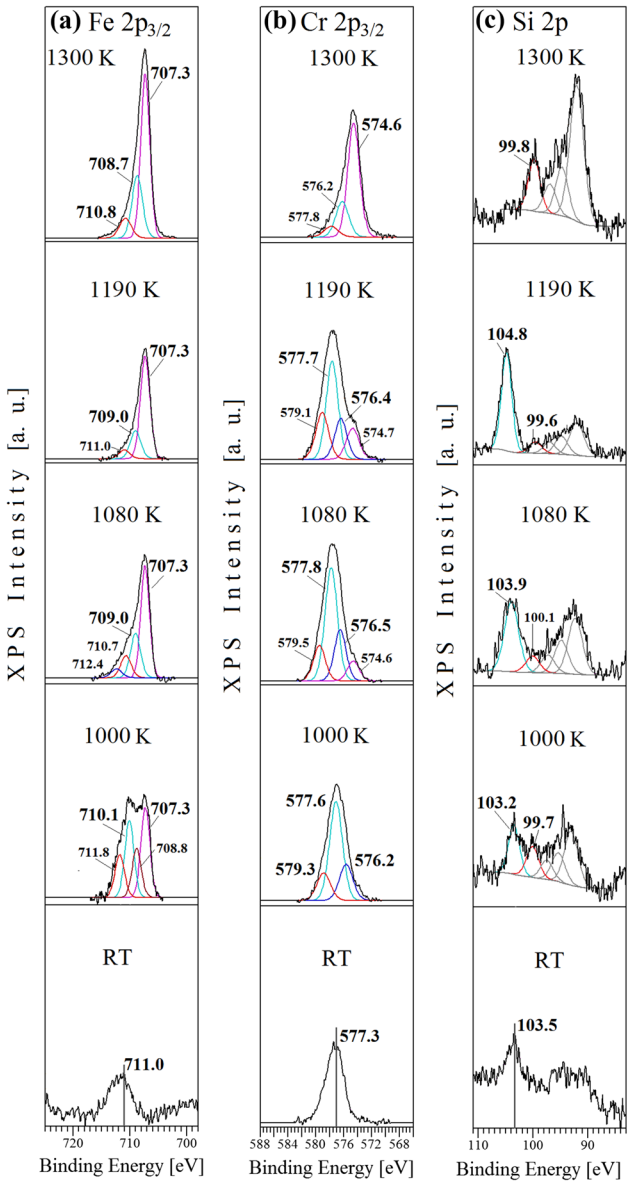

Fig. 10—(Color online) The selected XPS spectra for the $Fe_{0.90}Cr_{0.15}Si_{0.05}$ alloy after annealing at various temperatures: (*a*) Fe $2p_{3/2}$ peak, (*b*) Cr $2p_{3/2}$ peak, (*c*) Si 2p peak.

of both Cr and Si solutes. During the oxidation of samples with various initial Cr and Si bulk contents, the different passive films were formed. In the case of alloys with low chromium concentration ($Fe_{0.94}Cr_{0.03}Si_{0.03}$ and $Fe_{0.90}Cr_{0.05}Si_{0.05}$), only silicon segregation occurred and in the surface region only iron oxides, silicon oxides, and fayalite were observed. However, for the alloys with higher chromium concentration ($Fe_{0.85}Cr_{0.10}Si_{0.05}$ and $Fe_{0.80}Cr_{0.15}Si_{0.05}$), both solutes strongly segregate to the surface region, forming a protective passive layer, through which a significantly smaller amount of oxygen can penetrate the alloy (comparing with the oxidized film in other samples). The analysis of XPS spectra allows to distinguish iron, chromium, and silicon oxides, while no fayalite is detected. Annealing samples at high temperatures allows to obtain signal from the pure alloy elements. This fact could be also connected with good anti-corrosion properties of these alloys. Moreover, according to the obtained results the observed surface segregation process of Cr and Si atoms can be greatly enhanced by the presence of adsorbed oxygen atoms at the alloy surface. Therefore, the proper alloy preparation procedure with two additional stages, the initial low-temperature oxidation (for example, direct contact with air at RT) and subsequent annealing in vacuum at temperature lower than 1000 K, could lead to significant increase of corrosion resistance of the Fe-Cr-Si alloys with smaller bulk concentration of both solutes. This is extremely important since the high concentration of Cr and/or Si atoms in iron matrix often leads to the formation of brittle intermetallic phases and precipitates which reduces the mechanical properties of the prepared alloys. Finally, it should be noted that this type of material is relatively cheap and easy to produce and it can be widely used in the modern industry.

ACKNOWLEDGMENT

This work was supported by the Polish Ministry of Science and Higher Education under the "Iuventus Plus" programme in the years 2015-17, project number IP2014 015573.

REFERENCES

1. S. Khanna: *Introduction to High Temperature Oxidation and Corrosion*, Metals Park, OH, USA, ASM Int., 2002.
2. N. Birks, G.H. Meier, and F.S. Pettit: *Introduction to High Temperature Oxidation of Metals*, 2nd ed., Cambridge University, New York, NY, USA, 2006.
3. D. J. Young, *High Temperature Oxidation and Corrosion of Metals*, 2nd ed.; Elsevier Science, Amsterdam, 2016. ISBN: 978-0-08-100101-1.
4. S. Suzuki, T. Kosaka, H. Inoue, M. Isshiki, and Y. Waseda: *Appl. Surf. Sci.*, 1996, vol. 103, pp. 495–502, https://doi.org/10.1016/S0169-4332(96)00552-1.
5. V. Blum, A. Schmidt, W. Meier, L. Hammer, and K. Heinz: *J. Phys.: Condens. Matter*, 2003, vol. 15, pp. 3517–29, https://doi.org/10.1088/0953-8984/15/21/302.
6. I. Parezanowic and M. Spiegel: *Surf. Engineer.*, 2004, vol. 20, pp. 285–91, https://doi.org/10.1179/026708404225016517.
7. M. Vondracek, V. Dudr, N. Tsud, P. Lejcek, V. Chab, K.C. Prince, V. Matolin, and O. Schneeweiss: *Surf. Sci.*, 2006, vol. 600, pp. 4108–12, https://doi.org/10.1016/j.susc.2006.01.129.
8. A. Kiejna and E. Wachowicz: *Phys. Rev. B*, 2008, vol. 78, p. 113403, https://doi.org/10.1103/PhysRevB.78.113403.
9. S. Schonecker, S.K. Kwon, B. Johansson, and L. Vitos: *J. Phys. Condens. Matter*, 2013, vol. 13, p. 305002, https://doi.org/10.1088/0953-8984/25/30/305002.
10. R. Idczak, K. Idczak, and R. Konieczny: *J. Nucl. Mater.*, 2014, vol. 452, pp. 141–46, https://doi.org/10.1016/j.jnucmat.2014.05.003.
11. K. Idczak, R. Idczak, and R. Konieczny: *Physica B*, 2016, vol. 491, pp. 37–45, https://doi.org/10.1016/j.physb.2016.03.018.
12. R. Idczak, *Oxid. Met.*, 2017, vol. 87, pp. 75–88. 10.1007/s11085-016-9658-4.
13. R. Idczak: *Appl. Phys. A*, 2016, vol. 122, p. 1009, https://doi.org/10.1007/s00339-016-0544-3.
14. R. Idczak, K. Idczak, and R. Konieczny: *Physica B*, 2018, vol. 528, pp. 27–36, https://doi.org/10.1016/j.physb.2017.10.082.
15. R. Idczak, K. Idczak, and R. Konieczny: *Corrosion*, 2018, vol. 74, pp. 623–34, https://doi.org/10.5006/2676.
16. R. Idczak: *Corrosion*, 2018, vol. 74, pp. 1083–92, https://doi.org/10.5006/2776.
17. V. Crist: *Handbooks of Monochromatic XPS Spectra*, XPS International Inc., California, USA, The Elements and Native Oxides, 1999, vol. 1.
18. R. Idczak, R. Konieczny, and J. Chojcan: *J. Appl. Phys.*, 2014, vol. 115, p. 103513, https://doi.org/10.1063/1.4868471.
19. S. Cui and I.H. Jung: *Metall. Mater. Trans. A*, 2017, vol. 48A, pp. 4342–55, https://doi.org/10.1007/s11661-017-4163-1.
20. R.P. Gupta and S.K. Sen: *Phys. Rev. B.*, 1975, vol. 12, pp. 12–15, https://doi.org/10.1103/PhysRevB.12.15.
21. J.H. Scofield: *J. Electron Spectrosc.*, 1976, vol. 8, pp. 129–37, https://doi.org/10.1016/0368-2048(76)80015-1.
22. S. Tanuma, C.J. Powell, and D.R. Penn: *Surf. Interface Anal.*, 1994, vol. 21, pp. 165–76, https://doi.org/10.1002/sia.740210302.
23. A.P. Grosvenor, B.A. Kobe, M.C. Biesinger, and N.S. McIntyre: *Surf. Interace Anal.*, 2004, vol. 36, pp. 1564–74, https://doi.org/10.1002/sia.1984.
24. A. Idhil, C. N. Borca, A.-C. Uldry, N. Zema, S. Turchini, D. Catone, A. Foelske, D. Grolimund, M. Samaras, *Nucl. Instrum. Methods In Physics Research B,* 2012, vol. 284, pp. 1-5, https://doi.org/10.1016/j.nimb.2011.08.071.
25. S. Swaminathan and M. Spiegel: *Surf. Interface Anal.*, 2008, vol. 40, pp. 268–72, https://doi.org/10.1002/sia.2732.
26. M.C. Biesinger, B.P. Payne, A.P. Grosvenor, L.W.M. Lau, A.R. Gerson, and R.S.C. Smart: *Appl. Surf. Sci.*, 2011, vol. 257, pp. 2717–30, https://doi.org/10.1016/j.apsusc.2010.10.051.
27. T.D. Nguyen, J. Zhang, and D.J. Young: *Oxid. Met.*, 2014, vol. 81, pp. 549–74, https://doi.org/10.1007/s11085-013-9467-y.
28. M. Polak and B. Schiffmann: *J. Vac. Sci. Technol. A*, 1987, vol. 5, pp. 590–92, https://doi.org/10.1116/1.574679.
29. X. Tian, R.K.Y. Fu, L. Wang, and P.K. Chu: *Mater. Sci. Eng. A*, 2001, vol. 316, pp. 200–204, https://doi.org/10.1016/S0921-5093(01)01245-X.
30. M. Godec, D. Mandrino, B. Šuštaršič, and M. Jenko: *Surf. Interface Anal.*, 2002, vol. 34, pp. 346–51, https://doi.org/10.1002/sia.1314.
31. J. Moon, S. Kim, W.D. Park, T.Y. Kim, S.W. McAlpine, M.P. Short, J.H. Kim, and C.B. Bahn: *J. Nucl.*, 2019, vol. 513, pp. 297–308, https://doi.org/10.1016/j.jnucmat.2018.10.010.